The electronic structure of 4d and 5d silicides

Speier, W.; Kumar, L.; Sarma, D.D.; Groot, R.A. de; Fuggle, J.C.

Published in:
Journal of Physics%3A Condensed Matter

DOI:
10.1088/0953-8984/1/46/006

Publication date:
1989

J. Phys.: Condens. Matter **1** (1989) 9117–9129. Printed in the UK

The electronic structure of 4d and 5d silicides

W Speier†, L Kumar†‡, D D Sarma†§, R A de Groot‖ and J C Fuggle‖

† Institut für Festkörperforschung, Kernforschungsanlage Jülich, Postfach 1913, D-5170 Jülich, Federal Republic of Germany

‖ Research Institute for Materials, University of Nijmegen, Toernooiveld, 6525ED Nijmegen, The Netherlands

Received 24 February 1989

Abstract. A systematic experimental and theoretical study of the electronic structure of stoichiometric silicides with Nb, Mo, Ta and W is presented. We have employed x-ray photoemission and bremsstrahlung isochromat spectroscopy as experimental techniques and interpreted the measured data by calculation of the density of states and matrix elements for the compounds in their real crystal structures. Use is also made of x-ray emission spectra given in the literature. The electronic structure is analysed mainly in terms of the Si s, p and metal d states in relation to the various interactions, such as the metal–metal, metal–Si and Si–Si interaction. In discussing the trends of chemical bonding, we focus on the effect of the orbital overlap, the d-band occupancy and the composition.

1. Introduction

In this paper, we consider the electronic structure of some 4d and 5d silicides to the left in the series of transition-metal elements and, in a companion paper [1], we consider NiSi and NiAl as prototypes of compounds in which the transition-metal d band is nearly full. In a previous paper [2], we have considered the case of Ca silicides, where the d band is virtually empty. The electronic structure of silicides with transition metals can be related mainly to an interaction of orbitals with Si p and metal d symmetry ([3] and references therein). The underlying physical principle in the chemical bonding of transition-metal silicides is competition of the strong metal d–metal d interaction and the formation of metal d–Si p bonds (see, e.g., [1, 4]). The silicides with central 4d and 5d transition metals are a manifestation of these principles since they stabilise only in the extreme compositions of either metal-rich or silicon-rich compounds without an intermediate case. These two composition ranges exhibit also special features such as the occurrence of metal–metal distances in the metal-rich silicides which are much smaller than even those found in the pure elements and the occurrence of the very stable disilicides, which are attractive materials for the microelectronics industry (see, e.g., [5]).

As a result of the formation of bonding orbitals of mixed character, the relevant states involved in orbital interaction are distributed over an energy range of typically

‡ Permanent address: Physical Metallurgy Division, Bhabha Atomic Research Centre, Bombay 400085, India.

§ Permanent address: Solid State and Structural Chemistry Unit, Indian Institute of Science, Bangalore 560012, India.

0953-8984/89/469117 + 13 $02.50

20–25 eV around the Fermi level. Since the main information about the bonding interaction lies in the overall distribution of bonding and anti-bonding states, this necessitates a study of both the occupied and the unoccupied states. X-ray photoemission spectroscopy (XPS) and bremsstrahlung isochromat spectroscopy (BIS) provide two very useful spectroscopic techniques for this purpose since they give an immediate picture of the overall distribution of states with different symmetries and atomic sites and can be analysed in detail within the same theoretical framework [6].

However, the theoretical description of the electronic structure of silicides, based on band-structure calculations, is difficult owing to the complex crystal structure of most of these compounds. Accordingly, for early 4d and 5d silicides, calculated band structures in the real crystal structure exist so far only for $MoSi_2$ and WSi_2 [7]. Therefore, we have set out to calculate the electronic structure of all the silicides that we investigated in their actual crystal structures with a modern self-consistent band-structure scheme. By explicit calculation of the appropriate solid state matrix elements for XPS and BIS, we obtain a detailed picture of the experimental distribution of the site- and symmetry-selected density of states (DOS) in transition-metal silicides [8].

In this paper, we present our experimental and theoretical results on the electronic structure of transition-metal silicides of Nb, Mo, Ta and W in all their existing stoichiometric compositions. We discuss our results in terms of the chemical bonding and will emphasise the effect of orbital overlap, d-band occupancy and composition [9].

2. Experimental details

The polycrystalline samples were prepared by arc melting and indirect RF heating of metals and Si in the stoichiometric proportions in a cold crucible. The structures were checked by x-ray diffraction to be sure that no samples were used with more than 3% of spurious phases. The samples were cleaned by *in situ* scraping with a ceramic file at a vacuum of about 2×10^{-10} mbar.

The high-energy data were taken with combined XPS–BIS instruments with large-solid-angle (0.1 sr) XPS monochromators and a Pierce gun for BIS measurements. Cleanliness was checked using the C 1s, O 1s, metal and Si core-level XPS peaks, which showed that the impurity concentration was less than 0.25 monolayer both before and after valence band studies.

3. Computations

We used the augmented spherical-wave method as described in [10]. Scalar relativistic methods were included as described in [11]. Exchange and correlation effects were treated within the local-density approximation, as given in [12]. The basis sets included s, p and d functions on all sites, while the internal summation for the three-centre terms was carried out to one l-value higher than was included in the basis set. This means that f functions were included perturbatively. The radii of the Wigner–Seitz spheres were determined by equilibrating the overlap between them. The potential was iterated until self-consistency was achieved to a precision of $1{:}5 \times 10^{-5}$. As is usually the case with silicides, the calculations are extremely stable.

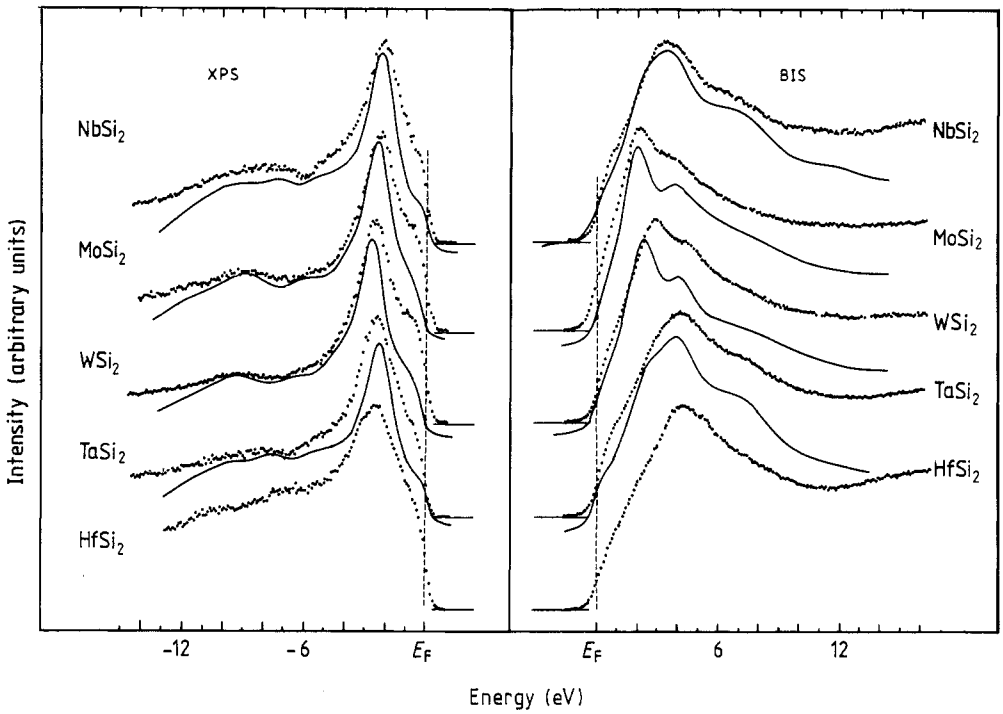

Figure 1. Experimental XPS and BIS spectra of the disilicides compared with the calculated spectral distribution. All spectra are normalised with respect to their maxima.

4. Results and interpretation

4.1. General overview

Figures 1 and 2 show our experimental and theoretical XPS–BIS results for the whole series of disilicides and metal-rich silicides. The calculated curves are constructed from the symmetry-projected partial DOS of inequivalent atomic sites in the unit cell, weighted by the appropriate matrix elements and broadened for lifetime effects and experimental resolution to allow direct comparison with the measured data. We find that the intensity distribution as obtained by the experiments is very well described by the theoretical spectra. All experimentally found spectral features are related to DOS effects and we find only small energy discrepancies of the order of 0.5 eV. The agreement is slightly better for the disilicides than for the metal-rich compounds, where some of the experimental features seem to have merged together although they are still distinguishable. Most important, all experimentally observed trends and changes from one compound to another can be followed in the theoretical curves and seem to be related to the specific composition or changes in the crystal structure. These effects are very pronounced for a comparison of the two series and are clearly visible by going from $NbSi_2$, $TaSi_2$ (C40 type) to $MoSi_2$, WSi_2 (CaC_2 type) or Mo_5Si_3, W_5Si_3 (T_1 type) to Nb_5Si_3 (T_2 type).

However, in order to relate these results to particular interactions, it is necessary to disentangle first the site- and symmetry-projected information in the total intensity distribution. This we do by concentrating on two representative examples, $NbSi_2$ in

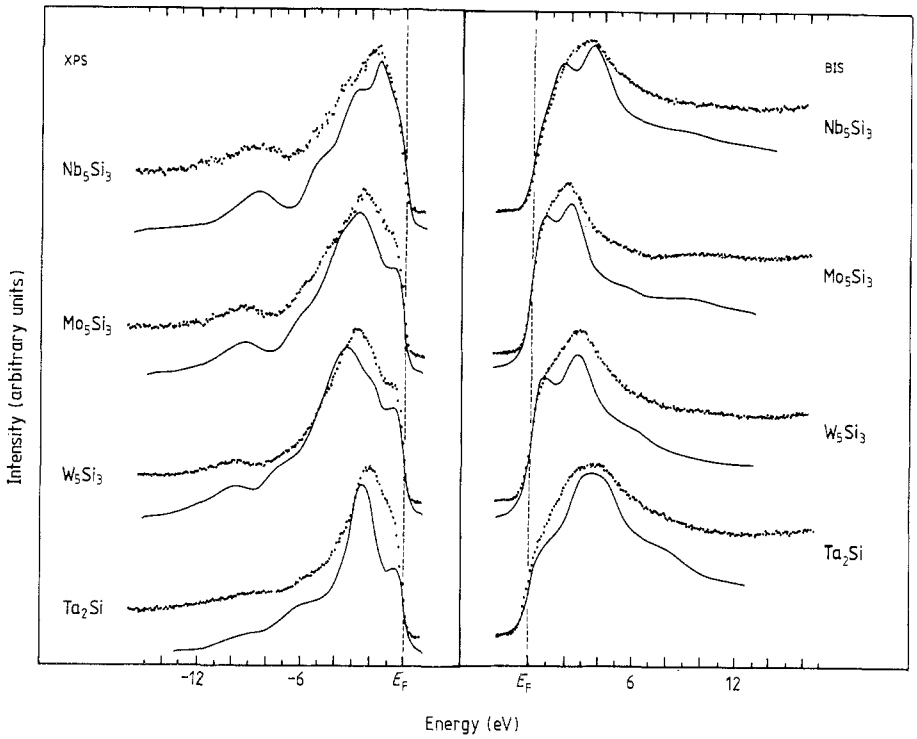

Figure 2. Experimental XPS and BIS spectra of the metal-rich silicides compared with the calculated spectral distribution. All spectra are normalised with respect to their maxima.

figure 3 and Ta_2Si in figure 4, which will serve as a basis for our interpretation of the whole series of disilicides and metal-rich silicides, respectively.

4.2. Disilicides

The effect of the matrix elements on the spectral distribution of the 4d and 5d disilicides is to enhance the contribution from states with Si s and metal d character with respect to those of Si p character [8]. This leads in the case of $NbSi_2$ in figure 3 to a clearly distinguishable Si s band from -7 to -12 eV binding energy, at the bottom of the valence states, and a major contribution of Nb d symmetry in the states around the Fermi level E_F between -5 and $+5$ eV. Otherwise the intensity shows a strong admixture of Si p states as reflected in the shoulder at 5 eV binding energy or at 7 eV above E_F. We observe at higher energies a decrease in intensity in the calculated BIS spectrum with respect to the DOS which is due to the suppression of the contribution of states with Si d symmetry by the matrix elements as a result of the centrifugal barrier [6].

These results are directly transferable to the whole series of disilicides that we have investigated (figure 1) by simply keeping in mind that the relative weight of metal d states will increase for the other compounds since Nb was the lightest transition metal in this series and the matrix elements for d states scales with the atomic number [6, 8]. With these results we can make an assignment of the states on the basis of the general bonding scheme of 4d and 5d silicides [7, 8, 13]. At the bottom of the valence bands, one finds the broad Si s bands, separated from the main structures. Then follow the Nb d

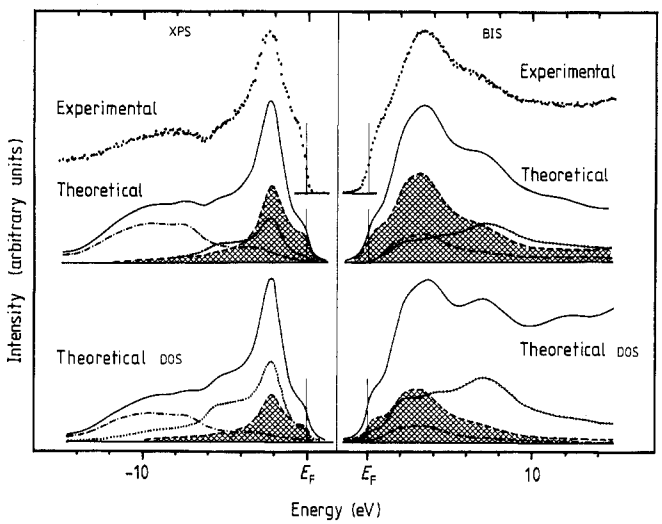

Figure 3. XPS and BIS spectra for $NbSi_2$ compared with the broadened DOS and the calculated spectra by including the matrix elements. The different contributions of Si s (—·—), Si p (·····) and Nb d (– – –) symmetry to the total DOS and spectral distribution are given. The experimental and theoretical spectra for the occupied and unoccupied part are normalised to the maxima. Note the strong redistribution of weight caused by the matrix elements for the Nb d states and the reduction in intensity in the BIS spectra at high energies due to a suppression of the Si d states.

and Si p states, which are mixed throughout the whole energy range up to 10 eV above E_F. The main contribution to the overall spectral shape arises from the bonding Nb d and Si p states centred around −2.5 eV and their anti-bonding counterparts around 2–4 eV above E_F with a region of low density of Si p states in between (often known as a 'quasi-gap'). Two aspects deserve special attention.

(i) The Si s band clearly has its main part separated from the main bonding–anti-bonding structures around E_F. By closer examination of the calculated DOS, we find that the Si s and p states form broad bands which overlap between about 4 and about 6 eV binding energy. This continuous crossover from s to p states can be observed experimentally in the Si, K and $L_{2,3}$ x-ray emission results [11, 13], which are closely

Table 1. Crystal structures for 4d and 5d silicides.

Material	Structure (type)	Symmetry group	References
$NbSi_2$	$CrSi_2$ (C40)	$P6_222$	[14, 15]
$MoSi_2$	$MoSi_2$ (CaC_2)	I4/mmm	[16]
$TaSi_2$	$CrSi_2$ (C40)	$P6_222$	[17]
WSi_2	$MoSi_2$ (CaC_2)	I4/mmm	[16]
Nb_5Si_3	T_2 (Cr_5B_3)	I4/mcm	[18]
Mo_5Si_3	T_1	I4/mcm	[19]
Ta_5Si_3	T_2 (Cr_5B_3)	I4/mcm	[18]
W_5Si_3	T_1	I4/mcm	[20]
Mo_3Si	A15	$Pm3n$	[21]
Ta_2Si	Al_2Cu	I4/mcm	[22]

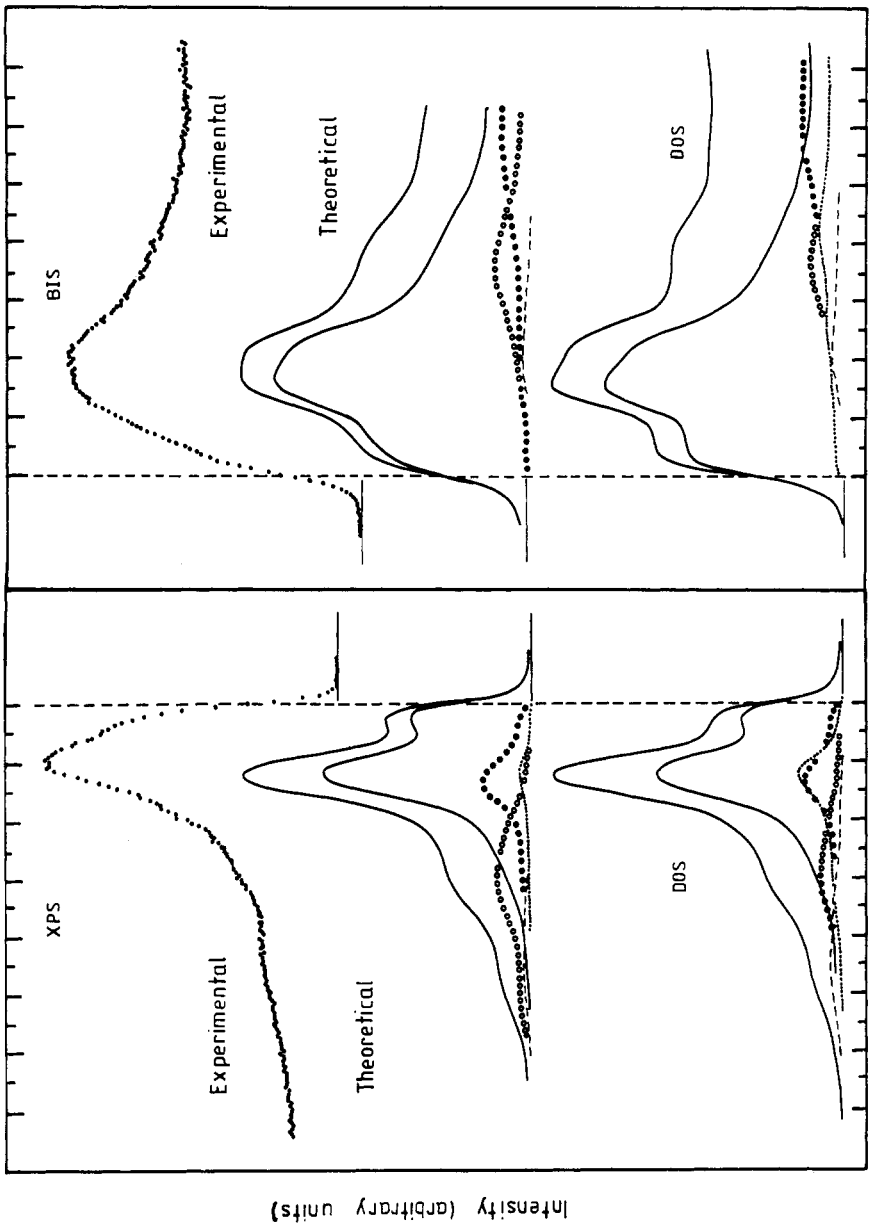

Figure 4. XPS and BIS spectra for Ta_5Si compared with the broadened DOS and the calculated spectra by including the matrix elements as in figure 1: ——, Ta d; ●●●●, Ta p; ○○○○○, Ta s; ·····, Si p; – – –, Si s.

related to the partial densities of, respectively, Si p and Si s(+d) states on the Si site. The broadening signifies direct Si–Si interaction. It is also interesting to note that the main Si s band varies in shape in connection with the change in crystal structure as we proceed from $NbSi_2$, $TaSi_2$ (C40 type) to $MoSi_2$, WSi_2 (CaC_2 type; see also table 1). The DOS clearly shows that there is also a considerable contribution of Si s character to the unoccupied states (around 2–5 eV above E_F). Together these results indicate that Si s states participate in the bonding interaction, in contrast with earlier schemes [3].

(ii) The metal d states are distributed over an energy range 18–20 eV owing to the interaction in the disilicides, although most of their weight is within ±5 eV of E_F. A major conclusion from our calculation is that we do not find any pure metal d character which could be ascribed to clearly distinguishable non-bonding states (compare with [3]) but rather a mixing with Si states, mainly of p character, throughout the whole energy range. Even the small structures in the quasi-gap, near the Fermi level in the unbroadened DOS, always have finite Si p character (see also [7]). This can be understood in terms of the large metal–metal distances in the disilicides, leading to a drastic reduction in the metal d–metal d interaction which would otherwise have led to a deeper quasi-gap.

Finally we again draw attention to the effects induced by the change in the crystal structure from one disilicide to another (table 1). The bonding states do not show an appreciable variation, as illustrated by our XPS data, and also earlier work using photoemission at a lower excitation energy [13]. However, a major redistribution of weight is seen in the unoccupied states, as illustrated by the BIS data in figure 1. The invariance of the occupied states is not in accordance with simple and band-filling arguments (rigid-band model). Inspection of the nearest-neighbour environment suggests that increasing the nuclear charge and providing an extra electron does not lead to a reduction in the nearest-neighbour distances, as for the pure elements, but is rather accompanied by a change in crystal structure in order to increase the coordination number, especially around Si. So, taking the unoccupied spectra into account, we become aware of characteristic spectral distributions for the particular crystal type, which is not obvious from a measurement of the occupied states alone.

4.3. Metal-rich compounds

Introduction of more metal atoms within the unit cell causes a dominance of metal-derived states in the DOS as well as in the experimental intensity distribution. By inspection of our experimental and theoretical results for Ta_2Si in figure 4 it becomes clear that the overall intensity is now almost completely determined by metal d states. Only at the bottom of the valence band, at around −10 eV, do we still observe the occurrence of a structure related to the Si s band, but with drastically reduced intensity. When the partial DOSs are weighted by the matrix elements, the intensity due to Si s symmetry is seen to overlap with the tail of the metal s states centred at approximately 6 eV in the calculation and probably gives rise to the shoulder at 5–6 eV in the XPS spectrum.

Another effect of the matrix elements is clearly observable in these data, namely the change in shape of the main d feature above the Fermi level which arises from the energy dependence of the XPS–BIS matrix elements. This behaviour is related to the embedding of the potential in the solid state surroundings and the induced change in spatial distribution of the wavefunctions by going from bonding to anti-bonding character [6].

Both results (the dominance of metal d states and mixture of Si s and metal s states at the bottom of the valence band) are directly transferable to the whole series of 5–3 compounds in figure 2 and the A15 compound, Mo_3Si (see figure 7). With these results we can give an assignment of structures in relation to the orbital interaction. The bonding interaction of metal d and Si p states causes a splitting of states centred around the Fermi level, in the case of Ta_2Si with bonding states concentrated between -5 and -1.5 eV below E_F and the anti-bonding counterpart at around 3–10 eV above E_F. In between these bands we find this time considerable metal d contribution around the Fermi level, situated in the quite distinct quasi-gap with a low density of Si p states. This is a general behaviour for early 4d or 5d metal-rich silicides as can already be recognised from the model calculation in [13].

Considering the different interactions here, we have the metal–Si interaction, which splits out the pd bonding and anti-bonding regions above and below the metal d states and the metal–metal interactions which broaden the metal d band. Because of the large spatial extent of the d wavefunctions, the metal d–metal d interaction is larger for the 4d and 5d series than for the 3d silicides. We note that the Si p DOS is almost negligible in the middle of the d band. Thus the strong metal–metal interactions not only broaden the metal d band but also push the bonding/anti-bonding metal/Si states apart and give rise to a well pronounced quasi-gap in the density of Si states. This is quite dramatic in the case of the 5/3 and A15 compounds, which exhibit nearest-neighbour metal–metal distances which are even smaller than in the pure elements, albeit with a lower coordination number (table 2). In this context it is interesting to observe that metal s and p states are mixed with Si s and p states. This indicates that the localisation of metal s and p symmetry into specific bonds play a key role in enabling the observed small metal–metal separations in compounds [4].

As in the case of the disilicides we observe for the metal-rich compounds distinct features for the specific crystal structure, by going from T_1 type (Mo_5Si_3 and W_5Si_3) to T_2 type (Nb_5Si_3 and Ta_5Si_3 (Ta_5Si_3 is not shown)). In these metal-rich silicides the crystal structure dependence is more pronounced and can be observed for the occupied as well as unoccupied states (figure 2).

Continuing, by comparison of the metal-rich silicides with the disilicides, we note that the width of the metal d band increases in the occupied part (except for Ta_2Si) and the XPS–BIS spectra exhibit a higher relative intensity at the Fermi level. Away from the Fermi level we observe more pronounced structures in the metal d DOS for the disilicides.

Table 2. Local atomic arrangements in $NbSi_2$ and $MoSi_2$. The number of neighbours at this distance is given in parentheses.

Atoms	Distances (Å)		
Nb–Si	2.60 (4)	2.77 (6)	
Si–Nb	2.60 (2)	2.77 (3)	
Nb–Nb			3.25 (4)
Si–Si	2.60 (2)	2.77 (3)	
Mo–Si	2.615 (8)	2.62 (2)	
Si–Mo	2.615 (4)	2.62 (2)	
Mo–Mo			3.2 (4)
Si–Si	2.615 (4)	2.62 (1)	3.2 (4)

Finally it should be pointed out that the Si s band at the bottom of the valence band narrows in going from the disilicides to the metal-rich compounds. This is also a quite general effect on dilution of Si [13, 23, 24]. This narrowing is observable in our XPS data (figures 1 and 2) as well as by x-ray emission [23, 25] and is due to decreased Si–Si contacts.

5. Discussion

5.1. General comments

The results, obtained by calculating the XPS–BIS spectra from the product of the partial DOSs and the matrix elements for the excitation process, give good agreement between experiment and theory. This indicates the absence of strong energy dependence of the self-energy and validates a detailed analysis of the different site- and symmetry-related contributions. In particular, we observe strong effects of the crystal structure and composition. As pointed out already in § 1, the silicides with the early 4d and 5d transition metals exhibit special crystal properties, which are not present in the 3d series. This includes the absence of the monosilicides as an intermediate composition, the change in crystal structure for both the metal-rich and the Si-rich compounds and finally the fact that only one A15 compound (Mo_3Si) exists for the early 4d and 5d silicides. This sum of macroscopic properties must be related mainly to the effect of increased overlap of the metal d states with its surroundings and to the delicate role of the d-band occupancy for stabilisation of certain crystal types. It is therefore instructive to try and disentangle the effects related to the hybridisation, d-band occupancy and composition.

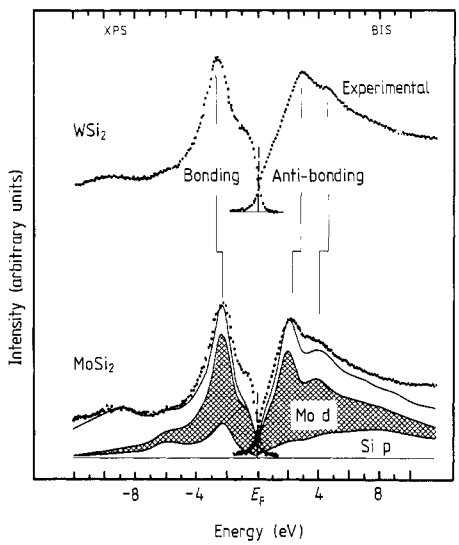

Figure 5. Illustration of the effect of the change in orbital overlap between metal d and Si p states in going from $MoSi_2$ to WSi_2. The relative intensities in the measured XPS–BIS spectra have been taken from the calculated curves. Also shown is the theoretical spectrum for $MoSi_2$ with the Si p and added metal d contribution (▒▒).

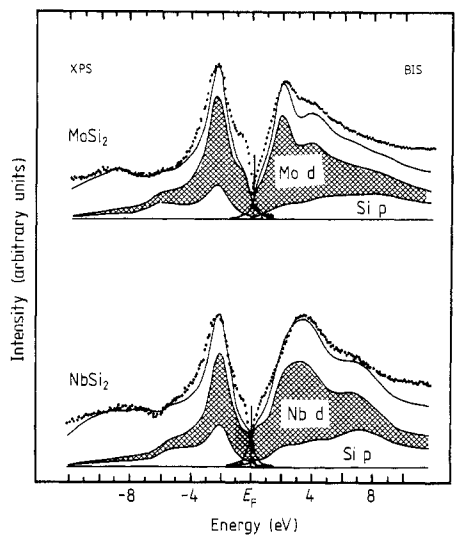

Figure 6. Illustration of the changes induced by the variation in d-band occupancy and crystal structure in going from $NbSi_2$ to $MoSi_2$. The relative intensities in the measured XPS–BIS spectra have been taken from the calculated curves which are shown together with their Si p and added metal d contributions (▒▒).

5.2. Effects of orbital overlap

An ideal example to study the changes induced by increased orbital overlap is the two compounds $MoSi_2$ and WSi_2 which have the same crystal structure with almost identical lattice parameters. In figure 5, we compare the XPS–BIS spectra of these compounds and emphasise again the bonding–anti-bonding mixing of metal d and Si p states in the calculated spectrum of $MoSi_2$. This overview reveals immediately the increase in energy separation of the bonding and anti-bonding states. This is precisely the effect that one would expect owing to an increased overlap of metal d and Si p orbitals as a consequence of larger spatial extension by going from the 4d to the 5d wavefunctions. Note that this increase in the splitting is also responsible for changes observed in optical data for these two compounds [26].

A closer examination of the metal d states as measured by photoemission [13, 27] and inverse photoemission [28] at lower excitation energies also confirms our finding that the relative intensity near E_F increases slightly with decreased overlap. This effect is even more obvious when going to the 3d series [13].

5.3. Effects of the d-band occupancy

The change in d-band occupancy introduced by going from the Nb, Ta group to the Mo, W group leads to changes in crystal structures. The case of the disilicides is particularly interesting since one observes a minor change in the occupied region but a major redistribution in the unoccupied states. This is illustrated in figure 6 for $NbSi_2$ and $MoSi_2$. Apart from the detailed form of the intensity distribution, the results show as a general effect a redistribution of the intensity of XPS with respect to BIS and a reduced splitting of the bonding–anti-bonding states.

Two effects should be considered then in the comparison of Nb and Mo silicides. First, the centre of the d band moves towards a higher binding energy. Secondly, the metal wavefunction contracts because of the increase in effective nuclear charge. These change the intensity distribution dramatically throughout the unoccupied states. As a

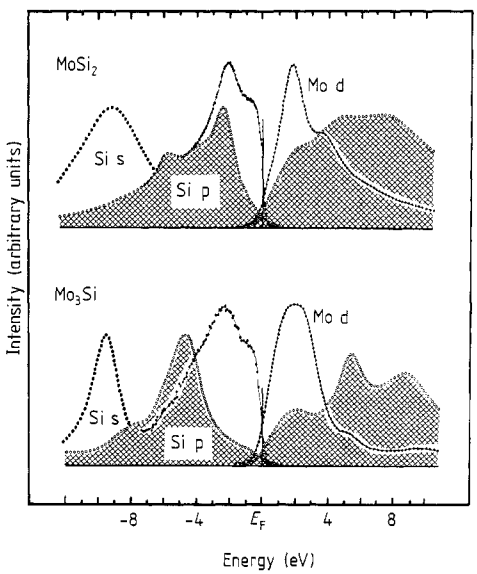

Figure 7. Illustration of the effect of composition by going from $MoSi_2$ to Mo_3Si. The different curves originate from experiments or theory. For the occupied Si s and p symmetry we used the x-ray emission results from [23]. The occupied metal d part is represented by photoemission data for a low excitation energy (50 eV) for $MoSi_2$ [24] and our x-ray energies for Mo_3Si. For the unoccupied part all the curves are calculated partial DOSS.

result of the change in occupancy, we observe in Mo silicides an overall increase in intensities for the occupied metal d states and a redistribution of states towards the Fermi level in the unoccupied states due to the reduced bonding/anti-bonding splitting. However, the contraction of the wavefunction does not lead to a decrease in the interatomic distances but rather to an increase in the coordination numbers (table 2). These changes in the atomic positions and coordination numbers determine, of course, the detailed form of the intensity distribution most prominent in the unoccupied d DOS. This also introduces a change in the Si p band in both the occupied (as observed for example in the high-binding-energy shoulder in the XPS spectra or the x-ray emission results in [25]) and the unoccupied states. In contrast with the disilicides we observe for the metal-rich compounds a general shift of structures in both the occupied and the unoccupied states.

5.4. Effects of composition

The electronic structure of 4d and 5d silicides is determined by a competing interplay of the direct metal d–metal d bonding and the metal d–Si p interaction [4]. The effect of these two different interactions can be seen by comparing the Si p and metal d distribution of states for $MoSi_2$ and Mo_3Si in figure 7. This is a composite picture in that we used experiments wherever they related directly to the specific symmetry and otherwise employed the partial DOS.

Experimental data for the occupied Si s and p states exist in the form of x-ray emission spectra which by excitation of atomic shells (1s in the case of the p DOS and 2p for the s DOS) provides the intensity distribution of the valence states originating from the Si sites [23]. The Mo d DOSs are closely related to those given by low-excitation-energy (about 70 eV) photoemission results [27] for $MoSi_2$ and by XPS for Mo_3Si because of the dominance of the metal d character. We do not possess the same direct information on the metal d and Si s or p states for the unoccupied states. The BIS intensity is strongly modified by other symmetries such as the metal s and p character and the Si p states are difficult to access by experiments since the inverse technique of x-ray emission, namely x-ray absorption, provides only information on the electronic states in the presence of an ionised atom, which distorts the local DOS [29]. We have thus used the calculated partial DOS. Also note that matrix elements distort the intensity distribution with respect to the DOS, which can be most clearly seen in the photoemission spectrum for $MoSi_2$ by comparing the intensity near E_F (figure 7) with the DOS (see figures 5 or 6).

From these data we learn that the bonding–anti-bonding Mo d–Si p bands in $MoSi_2$ change to a clearly separate region of Mo d character and Mo d–Si p states in Mo_3Si. We find strong Mo d bands situated around the Fermi level and broadened owing to the direct Mo–Mo interaction between Mo atoms along the chains of the A15 compounds. The bonding–anti-bonding Mo d–Si p states are grouped around this main Mo d band. By comparison with the XPS–BIS spectra for pure Mo, we realise that the overall width of the main Mo d band does not change appreciably by going to the Mo_3Si compound except for larger tails at both sides due to the additional Mo d–Si p interaction. This is no longer true for $MoSi_2$. This effect of a pile-up of DOS of Si p character at the edges of the main metal d band in the case of Mo_3Si is a general effect for the metal-rich silicides of early transition metals [13, 24]. This can be traced back [30] to the interaction of Si p states with the bonding and anti-bonding metal d bands. This leads in turn to a redistribution of states which is strongest at the bottom and top of the metal d bands. Our result shows that the Si p character groups sharply at the bottom of the d band but is spread over a wide energy range in the unoccupied part.

6. Conclusion

By use of the calculated DOS and the appropriate solid state matrix elements we are able to analyse XPS and BIS measurements of 4d and 5d transition-metal silicides in great detail. We found that the intensity distribution for the disilicides with 4d or 5d elements is mainly governed by states of Si s, p and metal d character. In the case of the metal-rich compounds the intensity of the spectra is almost completely determined by the metal-derived states, in particular of metal d symmetry. The spectral distribution of the stoichiometric compounds reflect the interplay of metal–metal, metal–Si and Si–Si interactions which govern the electronic structure of the silicides. In the case of the disilicides we observe a dominant metal d–Si sp bonding as well as direct Si–Si interaction and only a small contribution from metal–metal d interaction. In most metal-rich silicides we observe instead strong metal d–metal d interaction together with metal d–Si sp bonding. Spectroscopically the metal d–metal d interaction leads in the metal-rich compounds to pile-up of states of mainly metal d character around the Fermi level and the metal d–Si p bonding and anti-bonding states at both ends of the dominant metal d band. In the disilicides, these bonding and anti-bonding metal d–Si p states constitute the majority of all states, with the Fermi level situated in the 'quasi-gap'. The large spatial extension of the 4d and 5d wavefunctions and related orbital overlap with neighbouring sites gives rise to a large bonding–anti-bonding splitting and, in combination with the d occupancy, is responsible for the special crystal types of 4d and 5d silicides with respect to 3d silicides.

Our results indicate that the combination of XPS–BIS spectra exhibits an intensity distribution which is characteristic of the specific crystal type and composition. This could be used in principle as a 'fingerprint' in interface studies with early 4d and 5d transition metals which are of special importance in integrated-circuit manufacture.

Acknowledgments

We are grateful to M Campagna and W Gudat for encouragement in this work and S Krummacher for her contributions to setting it up. This work was supported financially by the Netherlands Foundation for Chemical Research (SON) with financial aid from the Netherlands Organisation for the Advancement of Research (NWO) and by the Netherlands Foundation for Fundamental Research (FOM).

References

[1] Sarma D D, Speier W, Zeller R, van Leuken E, Groot R A de and Fuggle J C 1989 *J. Phys. Condens. Matter* **1** 9131–9

[2] Sarma D D, Speier W, Kumar L, Carbone C, Spinsanti A, Bisi O, Iandelli A, Olcese G L and Palenzona A 1988 *Z. Phys.* B **71** 69

[3] Rubloff G W 1983 *Surf. Sci.* **132** 268
Calandra C, Bisi O and Ottoviani G 1985 *Surf. Sci. Rep.* **4** 271

[4] Williams A R, Gelatt C D, Connolly J W D and Moruzzi V L 1982 *Alloy Phase Diagrams*, ed. L H Bennett, J Massalski and M Griesse (Amsterdam: North-Holland) p 17

[5] Murarka S P 1983 *Ann. Rev. Mater. Sci.* **13** 117

[6] Speier W, Fuggle J C, Durham P, Blake R, Sterne P and Zeller R 1988 *J. Phys. C: Solid State Phys.* **21** 2621

[7] Bhattacharyya B K, Bylander D M and Kleinmann L 1985 *Phys. Rev.* B **32** 7973

[8] Speier W, van Leuken E, Fuggle J C, Sarma D D, Kumar L, Dauth B and Buschow K H 1989 *Phys. Rev.* B **39** 6008

[9] A complete diagnosis of chemical interaction involves a complicated analysis of the phases of the wavefunctions at all points in k–s space and of the overlap populations. Here we adopt a simplified procedure and assume that coincidence of peaks in the different partial DOSs indicates overlap or hybridisation of the levels involved. Whilst this procedure may not be foolproof when applied to a single system, it is unlikely to lead to serious errors when applied to a series of compounds with different structures.

[10] Williams A R, Kübler J and Gelatt C D 1979 *Phys. Rev.* B **19** 6094

[11] Methfessel M 1980 *Diplomarbeit* Ruhr Universität

[12] Hedin L and Lundqvist B I 1971 *J. Phys. C: Solid State Phys.* **4** 2064

[13] Weaver J H, Moruzzi V L and Schmidt F A 1981 *Phys. Rev.* B **23** 2916
Weaver J H, Franciosi A and Moruzzi V L 1984 *Phys. Rev.* B **29** 3293

[14] Trotter J (ed.), *Structure Reports, International Union of Crystallography* vol 38A (Utrecht: Oosthoek, Scheltema en Holkema) p 98

[15] Trotter J (ed.), *Structure Reports, International Union of Crystallography* vol 8 (Utrecht: Oosthoek) p 102

[16] Trotter J (ed.), *Structure Reports, International Union of Crystallography* vol 1 (New York: Johnson Reprint Corporation) p 783

[17] Trotter J (ed.), *Structure Reports, International Union of Crystallography* vol 8 (Utrecht: Oosthoek) p 102

[18] Trotter J (ed.), *Structure Reports, International Union of Crystallography* vol 19 (Utrecht: Oosthoek) p 279

[19] Trotter J (ed.), *Structure Reports, International Union of Crystallography* vol 19 (Utrecht: Oosthoek) p 278

[20] Trotter J (ed.), *Structure Reports, International Union of Crystallography* vol 19 (Utrecht: Oosthoek) p 277

[21] Trotter J (ed.), *Structure Reports, International Union of Crystallography* vol 12 (Utrecht: Oosthoek) p 111

[22] Trotter J (ed.), *Structure Reports, International Union of Crystallography* vol 38A (Utrecht: Oosthoek, Scheltema en Holkema) p 5

[23] Zaharowski W, Simunek A, Wiech G, Söldner K, Knauf R and Saemann-Ischenko G 1987 *J. Physique Coll.* C **9** 1025

[24] Bisi O and Chiao L W 1982 *Phys. Rev.* B **25** 4943
Franciosi A, Weaver J H, O'Neill D G, Schmidt F A, Bisi O and Calandra C 1983 *Phys. Rev.* B **28** 7000

[25] Zöpf E 1972 *PhD Thesis* Universität München

[26] Ferrieu F, Viguier C, Cros A, Humbert A, Thomas O, Madar R and Senateur J P 1987 *Solid State Commun.* **62** 455

[27] Weijs P 1988 private communication

[28] Baptist R 1988 private communication

[29] Kortboyer S, Grioni M, Speier W, Fuggle J C, Zeller R, Gibson M T, Watson L M and Schäfers F 1989 *J. Phys.: Condens. Matter* **1** 5981

[30] Pickett W E, Ho K M and Cohen M L 1979 *Phys. Rev.* B **19** 1734